Central European Journal of Economic Modelling and Econometrics

Dynamic Linkages in the Pairs (GBP/EUR, USD/EUR) and (GBP/USD, EUR/USD): How Do They Change During a Day?

Małgorzata Doman*, Ryszard Doman†

Submitted: 13.04.2014, Accepted: 19.05.2014

Abstract

In the paper, we document how conditional dependencies observed in the FOREX market change during a trading day. The analysis is performed for the pairs (GBP/EUR, USD/EUR) and (GBP/USD, EUR/USD) of exchange rates. We consider daily returns calculated using the exchange rates quoted at different hours of a day. The dynamics of the dependencies is modeled by means of 3-regime Markov regime switching copula models, and the strength of the linkages is described using dynamic Spearman's rho and the dynamic coefficients of tail dependence. The established approach allows us to monitor the changes in the dependence structure.

Keywords: exchange rates, FOREX, linkages, copula, Markov regime switching, Spearman's rho, volatility, tail dependence, crisis

JEL Classification: G15, C58, G01, C32

*Poznań University of Economics; e-mail: malgorzata.doman@ue.poznan.pl
†Adam Mickiewicz University in Poznań; e-mail: rydoman@amu.edu.pl

1 Introduction

In the paper, we document that the dynamics of linkages between the exchange rates for the pairs (GBP/EUR, USD/EUR) and (GBP/USD, EUR/USD) depends on time of a trading day. The analysis is based on daily returns calculated using the exchange rates quoted at 11 fixed hours of a day. To describe changes in a pattern of the linkages we apply 3-regime Markov regime switching copula models, and the strength of the dependencies is described using dynamic Spearman's rho and tail dependence coefficients.

The FOREX market is open 24 hours a day, with the exception of weekends. Trades between the FOREX participants are conducted through electronic communication networks and phone networks in various markets around the world. While some regional markets are closed, the other are open and the trade lasts. Trading hours of several regional markets overlap what results in more active FOREX trading during some periods. Figure 1 presents the periodic daily pattern observed in 5-minute returns of the exchange rate EUR/USD. The plot is obtained by calculating the average absolute value of the returns corresponding to each 5-minute segment. It is easy to observe that during a day there are three phases of higher volatility and thereby with higher market activity. The maxima visible in Figure 1 indicate the periods of the highest activity of traders from three main FOREX regions: Australia and Asia, Europe, and North America. The idea of our analysis comes from a conjecture that this pattern of changing activity should generate different patterns of conditional dependencies for daily returns built on exchange rates quoted at different times of a day. This is the reason why we perform our analysis of dependencies using daily returns calculated based on quotations from selected fixed hours of a day. Considering daily returns calculated in such a way seems to be quite natural in some circumstances. For instance, the daily returns calculated based on the quotations from 2:00 CET are strongly influenced by the activity of the Asian traders, and those corresponding to 9:00 CET can be considered as a result of decisions taken by the European traders. For investors from different continents different currencies are of importance, which should be reflected in the dynamics of dependencies. To the best of our knowledge, there are no earlier studies concerning the problem of changes in linkages in the FOREX market that take the proposed approach.

In Table 1, we show trading hours for the stock markets in the considered regions. Approximately, these periods are consistent with the periods of the most active trade in regional FOREX markets.

Our choice to model the dependencies for the pairs (GBP/EUR, USD/EUR) and (GBP/USD, EUR/USD) is connected with the idea of currency co-movement promoted by Eun and Lai (2004) and Eun et al. (2013). The investigation of co-movement in currency market is complicated because in order to describe the linkages between two currencies it is necessary to consider their exchange rates. Since the latter are calculated against a third currency, the results of the analysis strongly depend on the choice of it. Eun and Lai (2004) suggest that the exchange rates against the euro

Figure 1: EUR/USD. The daily periodic pattern in 5-minute returns (Central European Time). Calculations based on the observations from the period: November 11, 2011 — January 31, 2014

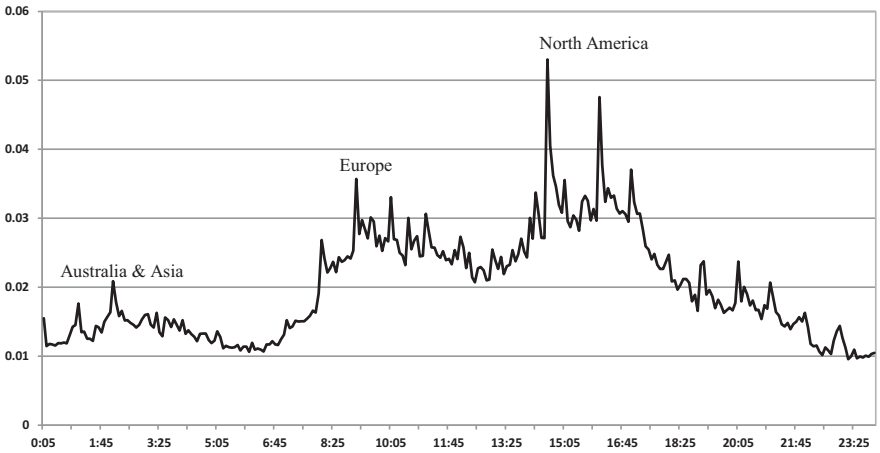

Table 1: A rough chart of trading hours for stock markets

CET																							
0	**1**	**2**	**3**	**4**	**5**	**6**	**7**	**8**	**9**	**10**	**11**	**12**	**13**	**14**	**15**	**16**	**17**	**18**	**19**	**20**	**21**	**22**	**23**
Australia																							
	Japan																						
		Singapore																					
					India																		
									Europe														
															USA								

should be used to describe linkages with the U.S. dollar, and, similarly, the exchange rates against the U.S. dollar should be applied to explain linkages with the euro. According to their philosophy, our analysis shows how the impacts of the U.S. dollar and the euro on the British pound change during the trading day in the FOREX market.

Our investigation covers the period from March 2, 2005 to January 31, 2014, and thus includes the long periods of financial crises and turmoil in global financial market. We are interested in possible changes in the structure of conditional dependencies which could be caused by these events. For this reason, our analysis is based on 3-regime Markov regime switching copula models, which are a tool flexible enough to capture qualitative and/or quantitative changes of the linkages in currency market. Applying this approach, we can measure not only the average conditional dependence using dynamic Spearman's rho coefficients, but, additionally, the obtained estimates of tail dependence coefficients enable us to get a deeper insight into the pattern of

the dependencies between extreme observations. In particular, due to applying the Markov regime switching copula models we are able to thoroughly trace temporal changes in the impact of the global currencies on the British pound during the period under scrutiny.
The results of our research are thus twofold. First, we show how the dynamic linkages between the GBP and the USD or the EUR are changing during the trading day. The second group of our results deals with those changes in the daily pattern of the dependencies which are caused by observed market events.

2 Copula-based dependence measures

It is well documented (McNeil et al. 2005) that outside the class of elliptical distributions (e.g. multivariate normal or multivariate Student's t) an adequate approach to measuring dependence between random variables should use the concept of a copula. A bivariate copula is a mapping $C : [0,1] \times [0,1] \to [0,1]$ from the unit square into the unit interval, which is a distribution function whose marginal distributions are standard uniform. The importance of copulas follows from a theorem by Sklar (1959). It states that if (X, Y) is a 2-dimensional random vector with joint distribution H and marginal distributions F and G then for some copula C the following formula holds:

$$H(x, y) = C\left(F(x), G(y)\right). \tag{1}$$

If F and G are continuous, the copula C is unique. It is called the copula of H or (X, Y), and can be represented as

$$C(u, v) = H\left(F^{\leftarrow}(u), G^{\leftarrow}(v)\right) \tag{2}$$

for $u, v \in [0,1]$, where $F^{\leftarrow}(u) = \inf\{x : F(x) \geq u\}$. It follows from (1) that by means of copula the marginals and the dependence structure can be separated. Thus, it makes sense to interpret the copula C as the dependence structure of the vector (X, Y).
The simplest copula is the one corresponding to independence of marginal distributions. It is defined by $C^{\Pi}(u, v) = uv$. In this paper we will also use the Gaussian, Joe-Clayton, and rotated Joe-Clayton copulas. They are defined as follows:

$$C_{\rho}^{Gauss}(u, v) = \Phi_{\rho}\left(\Phi^{-1}(u), \Phi^{-1}(v)\right), \tag{3}$$

$$C_{\kappa,\gamma}^{J-C}(u, v) = 1 - \left(1 - \left(\left[1 - (1-u)^{\kappa}\right]^{-\gamma} + \left[1 - (1-v)^{\kappa}\right]^{-\gamma} - 1\right)^{-1/\gamma}\right)^{1/\kappa}, \tag{4}$$

$$C_{\kappa,\gamma}^{J-C\_r90}(u, v) = v - C_{\kappa,\gamma}^{J-C}\left(1 - u, v\right). \tag{5}$$

In formula (3), Φ_{ρ} denotes the distribution function of a standard 2-dimensional normal vector with the linear correlation coefficient ρ, and Φ stands for the standard

normal distribution function.

The parameters of the Joe-Clayton copula (4) are assumed to satisfy the conditions: $\kappa \geq 1$, $\gamma > 0$. For $\kappa = 1$, the Joe-Clayton copula becomes the Clayton copula $C_{\gamma}^{Clayton}$. In the limit case $\gamma = 0$, the Clayton copula approaches the independent copula C^{Π} (Nelsen 2006). The rotated version of the Joe-Clayton copula, $C_{\kappa,\gamma}^{J-C\_r90}$, is applied to modeling negative dependence, which is impossible using the copula $C_{\kappa,\gamma}^{J-C}$.

An absolutely continuous copula C possesses the density c defined by

$$c(u,v) = \frac{\partial^2 C(u,v)}{\partial u \partial v}. \tag{6}$$

If H is an absolutely continuous distribution function with the copula C, the density c is related to the joint density function h by the following canonical representation:

$$h(x,y) = c\left(F(x), G(y)\right) f(x) g(y), \tag{7}$$

where F and G are the marginal distribution functions, and f and g are the marginal density functions.

Copula-based dependence measures are the ones that depend only on the copula of a random vector (X,Y). In particular, such measures are invariant with respect to strictly increasing transformations of the variables X or Y. In the case of non-elliptical random vectors they should be used instead of the linear correlation coefficient in order to avoid potential pitfalls (see, McNeil et al. 2005). An example of a copula-based dependence measure, which is used in the empirical part of this paper, is Spearman's rho. It is defined as

$$\rho_S(X,Y) = \rho\left(F(x), G(y)\right), \tag{8}$$

where F and G are the distribution functions of the variables X and Y, respectively (McNeil et al. 2005). If (X,Y) is a vector whose components have continuous distribution functions, and C is its copula, then

$$\rho_S(X,Y) = \rho_C = 12 \iint_{[0,1]^2} C(u,v)\, du dv - 3 \tag{9}$$

(Nelsen 2006). In the case of the Gaussian copula, C_{ρ}^{Gauss}, Spearman's rho equals $\frac{6}{\pi} \arcsin\left(\frac{1}{2}\rho\right)$ (McNeil et al. 2005). There is no explicit formula for Spearman's rho for the Clayton and Joe-Clayton copulas, so in this case one has to compute it numerically using (9). Spearman's rhos for the copula $C_{\kappa,\gamma}^{J-C\_r90}$ and $C_{\kappa,\gamma}^{J-C}$ differ only by the sign.

In financial applications, it is often very important to know whether two variables behave similarly when their extreme values occur. Such phenomena can be described in probabilistic terms by coefficients of tail dependence (see, Joe 1997). If X and Y are random variables with distribution functions F and G then the coefficient of

upper tail dependence is defined as

$$\lambda_{U,U} = \lim_{q \to 1^-} P\left(Y > G^{\leftarrow}(q) | X > F^{\leftarrow}(q)\right), \tag{10}$$

provided a limit $\lambda_{U,U} \in [0,1]$ exists. Analogously, the coefficient of lower tail dependence is defined as

$$\lambda_{L,L} = \lim_{q \to 0^+} P\left(Y \leq G^{\leftarrow}(q) | X \leq F^{\leftarrow}(q)\right), \tag{11}$$

provided that a limit $\lambda_{L,L} \in [0,1]$ exists. If $\lambda_{U,U} \in (0,1]$ ($\lambda_{L,L} \in (0,1]$), then X and Y are said to exhibit upper (lower) tail dependence. Upper (lower) tail dependence assesses the likelihood to observe a large (low) value of Y given a large (low) value of X. The coefficients of tail dependence are copula-based dependence measures: if C is the copula linking X and Y then

$$\lambda_{L,L} = \lim_{q \to 0^+} \frac{C(q,q)}{q}, \tag{12}$$

$$\lambda_{U,U} = \lim_{q \to 0^+} \frac{\hat{C}(q,q)}{q}. \tag{13}$$

where $\hat{C}(u,v) = u + v - 1 + C(1-u, 1-v)$. The Gaussian copula does not exhibit tail dependence: $\lambda_{U,U} = \lambda_{L,L} = 0$ (McNeil et al. 2005). In the case of the Joe-Clayton copula, $\lambda_{U,U} = 2 - 2^{1/\kappa}$and $\lambda_{L,L} = 2^{-1/\gamma}$ (Patton 2006), which means that upper and lower tail dependence coefficients are independent of each other.
When the components of the random vector (X,Y) display negative dependence the notion of negative tail dependence should be introduced. We define the coefficients of negative tail dependence, $\lambda_{U,L}$ and $\lambda_{L,U}$, by the following formulas:

$$\lambda_{U,L} = \lim_{q \to 0^+} P\left(Y \leq G^{\leftarrow}(q) | X > F^{\leftarrow}(1-q)\right), \tag{14}$$

$$\lambda_{L,U} = \lim_{q \to 1^-} P\left(Y > G^{\leftarrow}(q) | X \leq F^{\leftarrow}(1-q)\right), \tag{15}$$

provided that the limits exist. It can be directly shown that the coefficients of negative tail dependence depend solely on the copula C of the random vector (X,Y):

$$\lambda_{U,L} = \lim_{q \to 0^+} \frac{q - C(1-q,q)}{q}, \tag{16}$$

$$\lambda_{L,U} = \lim_{q \to 0^+} \frac{q - C(q,1-q)}{q}. \tag{17}$$

Moreover, formulas (5), (12), (13), (16) and (17) show that for the rotated Joe-Clayton copula $C^{J-C_r90}_{\kappa,\gamma}$the following holds:

$$\lambda_{U,L}\left(C^{J-C\_r90}_{\kappa,\gamma}\right) = \lambda_{L,L}\left(C^{J-C}_{\kappa,\gamma}\right) = 2^{-\frac{1}{\gamma}}, \tag{18}$$

$$\lambda_{L,U}\left(C^{J-C\_r90}_{\kappa,\gamma}\right) = \lambda_{U,U}\left(C^{J-C}_{\kappa,\gamma}\right) = 2 - 2^{\frac{1}{\kappa}}. \tag{19}$$

3 Markov regime switching copula models

When modeling time-varying joint conditional distributions of bivariate returns, the evolution of the conditional copula C_t has to be specified. Usually, the functional form of the conditional copula is fixed, but its parameters evolve through time (Patton 2004, 2006), or it is assumed that there are regimes in each of which a fixed copula prevails, and they switch according to some Markov chain (Garcia and Tsafack 2011). In the present paper, we follow the latter approach. Thus in the applied Markov regime switching copula model (MRSC model) the joint conditional distribution of the vector $r_t = (r_{1,t}, r_{2,t})$ has the following form

$$r_t|\Omega_{t-1} \sim C_{S_t}\left(F_{1,t}(\cdot), F_{2,t}(\cdot)|\Omega_{t-1}\right) \tag{20}$$

where S_t is a homogeneous Markov chain with state space $\{1,2,3\}$. The parameters of the MRSC model are the parameters of univariate models for marginal distributions (ARMA-GARCH), the parameters of copulas C_1, C_2 and C_3, and the transition probabilities, $p_{ij} = P\left(S_t = j|S_{t-1} = i\right)$, $(i,j) \in \{(1,1),(2,2),(3,3),(1,2),(2,1),(3,2)\}$.
The parameters of the model have been estimated by the maximum likelihood method. The main by-products of the estimation are the conditional probabilities $P\left(S_t = j|\Omega_{t-1}\right)$ and $P(S_t = j|\Omega_t)$, $j = 1,2,3$, which are calculated by means of Hamilton's filter (Hamilton 1994):

$$P\left(S_t = j|\Omega_{t-1}\right) = \sum_{i=1}^{3} p_{ij} P\left(S_{t-1} = i|\Omega_{t-1}\right), \tag{21}$$

$$P(S_t = j|\Omega_t) = \frac{c_j\left(u_t|S_t = j, \Omega_{t-1}\right)P(S_t = j|\Omega_{t-1})}{\sum_{i=1}^{3} c_i\left(u_t|S_t = i, \Omega_{t-1}\right)P(S_t = i|\Omega_{t-1})}, \tag{22}$$

where $p_{13} = 1 - p_{11} - p_{12}$, $p_{23} = 1 - p_{21} - p_{22}$, $p_{31} = 1 - p_{31} - p_{33}$, $u_t = (u_{1,t}, u_{2,t})'$,

$$u_{1,t} = F_{1,t}(r_{1,t}), \qquad u_{2,t} = F_{2,t}(r_{2,t}), \tag{23}$$

and $c_j\left(\cdot|S_t = j, \Omega_{t-1}\right)$ is the density of the conditional copula coupling the conditional marginal distributions in regime j, $j = 1,2,3$. The maximized log-likelihood function has the form

$$\begin{aligned} L \;=\; & \sum_{t=1}^{T} \ln\left(\sum_{j=1}^{3} c_j\left(u_t|S_t = j, \Omega_{t-1}; \tilde{\theta}_j\right) P\left(S_t = j|\Omega_{t-1}; \tilde{\theta}_j\right)\right) + \\ & + \sum_{t=1}^{T} \ln\left(f_{1,t}\left(r_{1,t}|\Omega_{t-1}; \theta_1\right)\right) + \sum_{t=1}^{T} \ln\left(f_{2,t}\left(r_{2,t}|\Omega_{t-1}; \theta_2\right)\right) \end{aligned}, \tag{24}$$

where $f_{1,t}$ and $f_{2,t}$are the density functions corresponding to $F_{1,t}$ and $F_{2,t}$, fitted using the AR-GARCH models.

When presenting the empirical results, we use the so-called smoothed probabilities. They are calculated from the predicted and filtered probabilities by using the backward recursion:

$$P\left(S_t = j|\Omega_T\right) = P\left(S_t = j|\Omega_t\right) \sum_{i=1}^{3} \frac{p_{ji} P\left(S_{t+1} = i|\Omega_T\right)}{P\left(S_{t+1} = i|\Omega_t\right)}, \quad t = T-1, \ldots, 1, \tag{25}$$

where T denotes the length of the sample.
The models are estimated by the two-step maximum likelihood method. Thus, first we fit univariate ARMA-GARCH models to the return data. Then, the obtained standardized residuals are transformed to uniform variates, using the theoretical cumulative distribution functions. After that, the Markov regime switching copula models are fitted and estimates of dynamic Spearman's rho and the lower and upper tail coefficients and the coefficients of negative tail dependence are calculated using the smoothed probabilities.
The above approach to estimating copula-based models has an advantage that it is computationally tractable at a moderate cost of the loss of full efficiency (Patton 2012, 2013). As an alternative approach, Bayesian inference should be mentioned (see e.g. Min and Czado 2010, Almeida and Czado 2012, and references therein). The latter includes uncertainty of the parameter estimates and can deliver credible intervals for the time-varying point estimates of Spearman's rho.

4 The Model Confidence Set

The Model Confidence Set (MCS) methodology was introduced by Hansen et al. (2003). It was originally designed for selecting the best volatility forecasting models. Its applications, however, are not limited to evaluation of models. Equally well, it can be used to compare the means of two or more populations. The MCS procedure allows to select in a set of models a subset consisting of models which are better than the others in terms of some specified criterion. To be precise, for some collection $\mathcal{M}^0$of models, the MCS procedure produces a subset $\hat{\mathcal{M}}^*_{1-\alpha}$ of $\mathcal{M}^0$, which contains the subset$\mathcal{M}^*$ of superior models with a given confidence level $1-\alpha$. The collection $\mathcal{M}^0$ can be any finite set of objects indexed by $i = 1, \ldots, m_0$. Suppose they are evaluated in terms of a loss function that assigns to the object i in period t the loss $L_{i,t}$, $t = 1, \ldots, n$. If the relative performance is defined as $d_{ij,t} \equiv L_{i,t} - L_{j,t}$ for $i, j \in \mathcal{M}^0$ and the mean $\mu_{ij} \equiv E\left(d_{ij,t}\right)$ is finite and does not depend on t, then the set of superior objects is defined by

$$\mathcal{M}^* \equiv \left\{i \in \mathcal{M}^0 : \ \mu_{ij} \leq 0 \text{ for all } j \in \mathcal{M}^0\right\}.$$

The MCS procedure uses an equivalence test $\delta_{\mathcal{M}}$ to test the hypothesis

$$H_{0,\mathcal{M}} : \ \mu_{ij} = 0 \text{ for all } i, j \in \mathcal{M},$$

at level α for any $\mathcal{M} \subset \mathcal{M}^0$. When $H_{0,\mathcal{M}}$ is rejected, an elimination rule $e_{\mathcal{M}}$ is applied to identify the object of $\mathcal{M}$ that is to be removed from $\mathcal{M}$. Consequently, the MCS is based on the following steps:

Step 0: Set initially $\mathcal{M} = \mathcal{M}^0$.

Step 1: Test $H_{0,\mathcal{M}}$ at significance level α using $\delta_{\mathcal{M}}$.

Step 2: If $H_{0,\mathcal{M}}$ is not rejected, set $\hat{\mathcal{M}}^*_{1-\alpha} = \mathcal{M}$, otherwise use $e_{\mathcal{M}}$ to eliminate an object from $\mathcal{M}$ and repeat the procedure beginning with Step 1.

It is proved in Hansen et al. (2011) that under some standard requirements for the equivalence test and the elimination rule it holds that

$$\lim_{n\to\infty} \inf P\left(\mathcal{M}^* \subset \hat{\mathcal{M}}^*_{1-\alpha}\right) \geq 1-\alpha, \tag{26}$$

$$\lim_{n\to\infty} P\left(i \in \hat{\mathcal{M}}^*_{1-\alpha}\right) = 0 \text{ for all } i \notin \mathcal{M}^*, \tag{27}$$

$$\lim_{n\to\infty} P\left(\mathcal{M}^* = \hat{\mathcal{M}}^*_{1-\alpha}\right) = 1 \text{ if } \mathcal{M}^* \text{ consists of a single model.} \tag{28}$$

The MCS p-values are defined as follows. If $P_{H_0,\mathcal{M}_i}$ denotes the p-value associated with the null hypothesis $H_{0,\mathcal{M}_i}$ (with convention that $P_{H_0,\mathcal{M}_{m_0}} = 1$), then the MCS p-value for model $e_{\mathcal{M}_j} \in \mathcal{M}^0$ is defined as $\hat{p}_{e_{\mathcal{M}_j}} \equiv \max_{i\leq j} P_{H_0,\mathcal{M}_i}$.

The null hypothesis $H_{0,\mathcal{M}}$ can be tested using traditional quadratic-form statistics or multiple t-statistics (see, Hansen et al. 2011). In this paper, we apply the t-statistic $T_{R,\mathcal{M}}$ defined as

$$T_{R,\mathcal{M}} = \max_{i,j\in\mathcal{M}} |t_{ij}|, \tag{29}$$

where

$$t_{ij} = \frac{\bar{d}_{ij}}{\sqrt{v\hat{a}r\left(\bar{d}_{ij}\right)}} \text{ for } i,j \in \mathcal{M}, \tag{30}$$

and $\bar{d}_{ij} = n^{-1}\sum_{t=1}^{n} d_{ij,t}$. Because of the presence of nuisance parameters, the asymptotic distribution of the statistic $T_{R,\mathcal{M}}$ is nonstandard. The bootstrap implementation of the MCS procedure involving this statistic is described in Appendix B of the paper by Hansen et al. (2003). The estimated bootstrap distribution of $T_{R,\mathcal{M}}$, under the null hypothesis, is given by the empirical distribution of

$$T^*_{b,R} = \max_{i,j\in\mathcal{M}} \frac{|\bar{d}^*_{b,ij} - \bar{d}_{ij}|}{\sqrt{\widehat{\text{var}}\left(\bar{d}_{ij}\right)}}, \tag{31}$$

where $\bar{d}^*_{b,ij} = \frac{1}{n}\sum_{t=1}^{n} d_{ij,\tau_{b_t}}$ is the bootstrap resample average, and $\widehat{\text{var}}\left(\bar{d}_{ij}\right) = \frac{1}{B}\sum_{b=1}^{B}\left(\bar{d}^*_{b,ij} - \bar{d}_{ij}\right)^2$. For generating B resamples, the block bootstrap is used. The p-value of $H_{0,\mathcal{M}}$ is given by

$$P_{H_{0,\mathcal{M}}} = \frac{1}{B}\sum_{b=1}^{B} \mathbf{1}\left\{T^*_{b,R} > T_{R,\mathcal{M}}\right\}. \tag{32}$$

In the present paper, we apply the MCS procedure to compare the means of exchange rate volatilities, and the averages of strength of linkages between exchange rates, measured by means of Spearman's rho.

5 The data

We investigate the exchange rates GBP/USD, GBP/EUR and EUR/USD. As it is established in the practice of FX markets, the symbol X/Y means the price of a unit of the currency X in units of the currency Y. The analysis is performed for the daily percentage logarithmic returns, which are separately calculated based on exchange rates quoted at 11 fixed hours of a day: 2:00 CET, 4:00 CET, 6:00 CET , . . . , 22:00 CET. The period under scrutiny is from March 2, 2005 to January 31, 2014 (2317 daily observations for each of the selected hours). The exchange rate series were obtained from the service Stooq. The plots in Figure 2 present the quotations, over the period under scrutiny, of the exchange rate GBP/EUR at indicated hours of a day. The fluctuations of the quotations of the GBP/EUR at the selected hours of the same day are not very strong, and similar behavior has been observed in the case of the other analyzed exchange rates.

Figure 2: The quotations of the exchange rate GBP/EUR at 4.00, 10.00, 14.00, 16.00. 22.00 CET

6 Analysis of volatility and dependencies

To investigate dependencies between the analyzed exchange rates, we use 3-regime Markov switching copula models. This allows us to describe different types of dependence and capture temporal changes in the linkages of the GBP with the USD or the EUR.

As mentioned in Section 3, we applied a 2-step estimation procedure. First, we fitted a univariate ARMA-GARCH model to each of the investigated return series. As usually in the case of very liquid assets, the fitted models are mostly simple GARCH or GJR-GARCH with a Student's t or skewed Student's t distribution for the innovations (Tsay 2010). The standardized residuals from the fitted ARMA-GARCH models were examined for consistency with the assumed distributional properties and serial independence. Next, they were transformed by means of the theoretical cumulative distribution functions into the series of the form (23), and the MRSC models were fitted by the maximum likelihood method, using the first summand in (24). We considered copulas from various families including those allowing to capture negative dependence. In the final choice we followed the results of the information criteria and the likelihood ratio tests performed where they were applicable. The estimation was done using G@RCH 6.0 package (Laurent 2009) and the Matlab software.

The first part of our results concerns the dynamics of volatility. Due to space limitations, we do not report here full results of the estimation of univariate models. Table 2 contains the types of GARCH models fitted to the analyzed data. In Figures 3-8, the corresponding volatility estimates are shown.

Table 2 shows that the dynamics of the daily exchange rate returns is changing over the day. Interesting things are appearance and disappearance of asymmetry in the data and changes in the number of degree of freedom (DF) in Student's t distribution. A lower DF value means more frequent occurrence of outliers in the return process. This indicates higher market sensitivity on new information and is connected with more active trading. In the case of the EUR/USD, the highest DF values are observed from 2:00 CET to 8:00 CET. This is a time period when the European and the U.S. markets are closed. At the same time, we observe the lowest DF values for the GBP/USD. This means that for Asian traders the latter exchange rate is more important than the former. The GBP/EUR is the most heavily traded when the European markets are open (9:00 CET – 17:00 CET). There are only four cases with skewed Student's t distribution (negative asymmetry) for the innovations: EUR/USD (at 10:00 CET and 14:00 CET) and GBP/USD (at 16:00 CET and 20:00 CET).

When the fitted models are GJR-GARCH or APARCH, we meet another type of asymmetry connected with the so-called leverage effect (see, Tsay 2010). From Tables 1 and 2 it is easy to see that in the case of the GBP/EUR returns this type of asymmetry is produced by joint activity of Asian markets (in particular Indian markets) and the U.S. markets. The GBP/USD daily returns show asymmetric behavior for all the considered hours with the exception of 10:00 CET (joint impact of Asian and European markets). The best model for the EUR/USD data is mostly a

GARCH(1,1). The asymmetric phenomena are present at 2:00 CET, 8:00 CET, 12:00 CET (model), 10.00 CET (distribution) and 14:00 CET (model and distribution).

Table 2: Types of GARCH models fitted to daily returns calculated for data quoted at the selected hours

Time		Model	Error distribution	DF
02:00 CET	GBP/EUR	GARCH(1,1)	Student's t	10.3596
	GBP/USD	APARCH(1,1)	Student's t	12.3200
	EUR/USD	GJR(1,1)	Student's t	17.1611
04:00 CET	GBP/EUR	GARCH(1,1)	Student's t	10.4833
	GBP/USD	GJR(1,1)	Student's t	9.8004
	EUR/USD	GARCH(1,1)	Student's t	19.3057
06:00 CET	GBP/EUR	GJR(1,1)	Student's t	12.4250
	GBP/USD	GJR(1,1)	Student's t	8.7681
	EUR/USD	GARCH(1,1)	Student's t	17.2284
08:00 CET	GBP/EUR	GJR(1,1)	Student's t	11.8465
	GBP/USD	APARCH(1,1)	Student's t	11.6859
	EUR/USD	APARCH(1,1)	Student's t	18.3356
10:00 CET	GBP/EUR	GARCH(1,1)	Student's t	8.4246
	GBP/USD	GARCH(1,1)	Student's t	15.2273
	EUR/USD	GJR(1,1)	skewed Student's t	10.8435
12:00 CET	GBP/EUR	APARCH(1,1)	Student's t	9.0222
	GBP/USD	APARCH(1,1)	Student's t	11.7500
	EUR/USD	GJR(1,1)	skewed Student's t	10.8229
14:00 CET	GBP/EUR	GARCH(1,1)	Student's t	9.5010
	GBP/USD	APARCH(1,1)	Student's t	14.6261
	EUR/USD	GJR(1,1)	skewed Student's t	9.7261
16:00 CET	GBP/EUR	GJR(1,1)	Student's t	11.8611
	GBP/USD	GJR(1,1)	skewed Student's t	15.0727
	EUR/USD	GARCH(1,1)	Student's t	9.3614
18:00 CET	GBP/EUR	GJR(1,1)	Student's t	10.2973
	GBP/USD	GJR(1,1)	Student's t	18.2761
	EUR/USD	GJR(1,2)	Student's t	10.3879
20:00 CET	GBP/EUR	GJR(1,1)	Student's t	11.5533
	GBP/USD	GJR(1,1)	skewed Student's t	19.2365
	EUR/USD	GARCH(1,2)	Student's t	12.4385
22:00 CET	GBP/EUR	GARCH(1,1)	Student's t	13.7302
	GBP/USD	APARCH(1,1)	Student's t	10.8207
	EUR/USD	GARCH(1,1)	Student's t	16.7874

The models described in Table 2 are simple, but they indicate some changes in the dynamics of volatility when different hours of a day are considered. These diverse models, however, give very similar volatility estimates. This is clearly visible in Figures 3-5 presenting volatility estimates for the exchange rates quoted at 4:00 CET, 10:00 CET, 14:00 CET, 16:00 CET and 22:00 CET. All the plots show a well-known

volatility pattern. The explosion of volatility corresponds in each case to the short period during the subprime crisis encompassing the bankruptcy of Lehman Brothers. The main observation is that the daily volatility estimates corresponding to different hours do not differ significantly. This impression is confirmed by the plots in Figures 6-8 presenting a synthetic view on the volatility estimates.

The surfaces presented in Figures 6-8 show that generally the level of volatility remains almost unchanged across the selected hours of a day. Some fluctuations, however, are observed during turmoil periods – the strongest during the subprime crisis and weaker in time of the Eurozone crisis. This indicates a higher market sensibility on information during the crisis period.

The main part of our analysis deals with the question about the changes in the conditional dependence structure connected with the activity of different regional markets. In Table 3 we present the types of all fitted MRSC models, and in Tables 4-6, examples of parameter estimates are given. In the case of the pair (GBP/USD, EUR/USD) we do not observe tail dependence. The fitted models are 3 or 2-regime MRSC ones with two Gaussian copulas and the independence copula in the case where regime 3 appears. The number of regimes changes depending on the considered hour of a day. The dynamics of linkages between the GBP/EUR and USD/EUR is more complicated. Usually, in one of the regimes the Joe-Clayton copula prevails, indicating the presence of lower and upper tail dependencies. The only exceptions are 8:00 CET (before European markets opening) and 22:00 CET (the U.S. market closing).

Table 3: The types of MRSC models fitted to daily returns calculated for data quoted at the selected hours

Time	02:00	04:00	06:00	08:00	10:00	12:00	14:00	16:00	18:00	20:00	22:00
GBP/EUR-USD/EUR	G-G-JC	JC-JC	G-G-JC	G-G	JC-JC	G-G-JC	G-G-JC	G-G-JC	G-G-JC	G-G-JC	G-G
GBP/USD-EUR/USD	G-G-Π	G-G	G-G	G-G-Π	G-G	G-G	G-G-Π	G-G-Π	G-G	G-G-Π	G-G-Π

Tables 4-6 present parameter estimates for MRSC models fitted to daily returns calculated for the data quoted at 16:00 CET, 10:00 CET, and 6:00 CET. The chosen models fit the data well. Gaussian copulas describing dependence in different regimes differ by their correlation coefficients, indicating stronger or weaker dependence. The matrices of transition probabilities show that regimes are distinguished properly. The observed dependencies are strong, so there was no doubt about the choice of the best model.

Figure 9 presents estimates for dynamic Spearman's rho for (GBP/USD, EUR/USD). The dynamics changes with the considered hours of a day. The most stable linkages correspond to 4:00 CET and 10:00 CET. Spectacular drops in the strength of dependence occur during the periods of turmoil in financial markets. An interesting observation is that during the periods of crisis the value of Spearman's rho decreases even to 0, indicating temporary conditional independence. The surface of dynamic

Figure 3: GBP/EUR. Daily volatility estimates corresponding to different hours

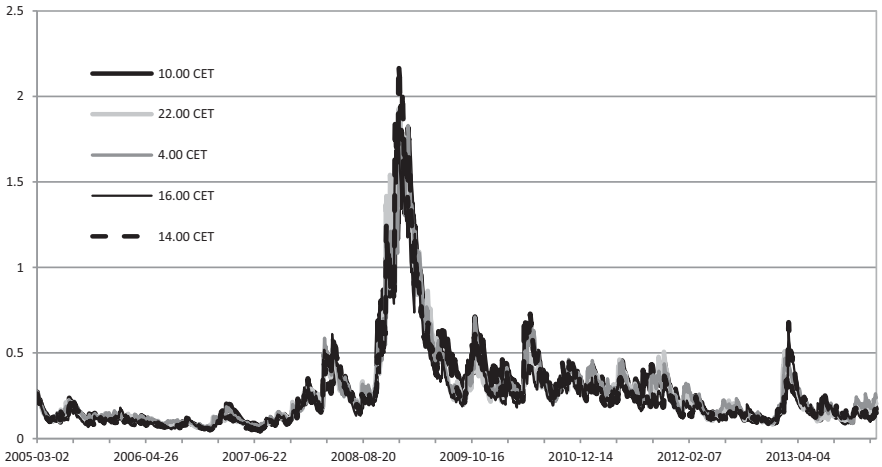

Figure 4: GBP/USD. Daily volatility estimates corresponding to different hours

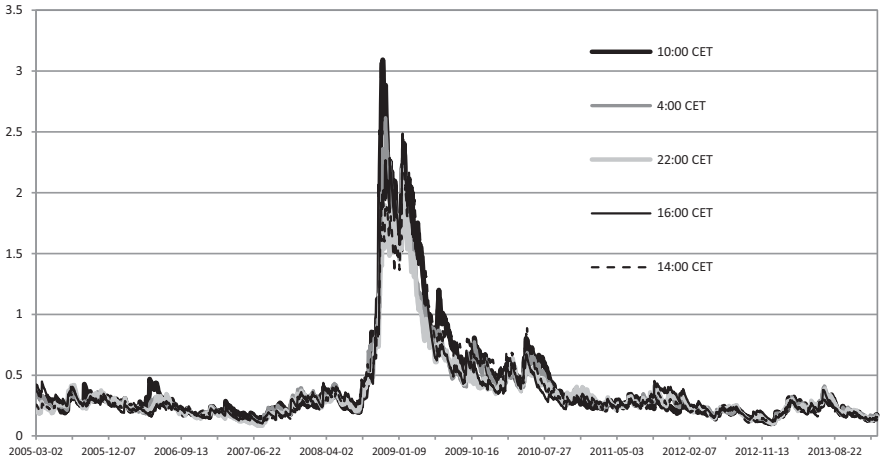

Spearman's rhos in Figure 10 confirms the above remarks.
The MRSC models fitted to (GBP/EUR, USD/EUR) are more complicated than those for (GBP/USD, EUR/USD). However, the dynamics of Spearman's rho presented in Figures 11-12 seems to be less sensitive on markets events. The Spearman's rho estimates are lower but more stable. The periods of sharp increase are connected with crises in the USA and in the Eurozone. The plot in Figure 12, however, shows that even during calm periods conditional dependence between GBP/EUR and

Figure 5: EUR/USD. Daily volatility estimates corresponding to different hours

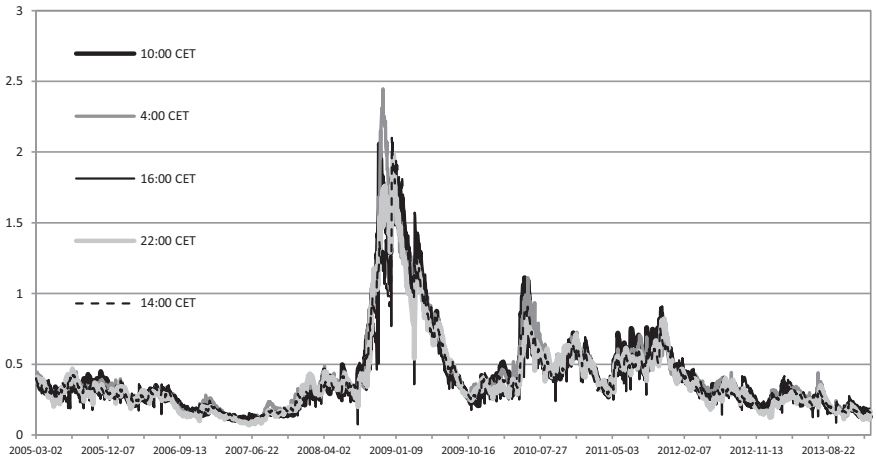

Figure 6: GBP/EUR. Surface of volatilities

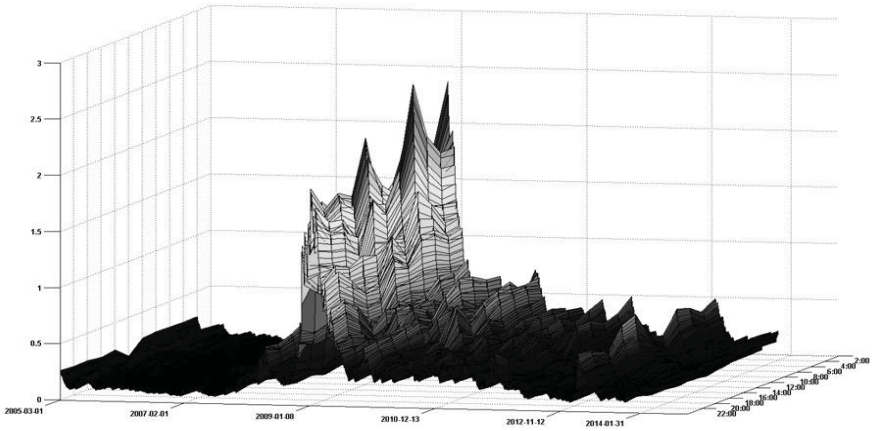

USD/EUR changes with the considered hours of a day.

In Figure 13 we present estimates of the dynamic coefficients of lower tail dependence for the pair (GBP/EUR, USD/EUR). The dynamics is similar to that visible in Figure 11. The main observation is that lower tail dependence appears in crisis periods (the subprime crisis and the Eurozone crisis).

In the last part of the analysis we use the MCS methodology to compare the averages of strength of linkages measured by means of Spearman's rho obtained for pairs of daily returns corresponding to the considered hours of a day. A similar comparison

Figure 7: GBP/USD. Surface of volatilities

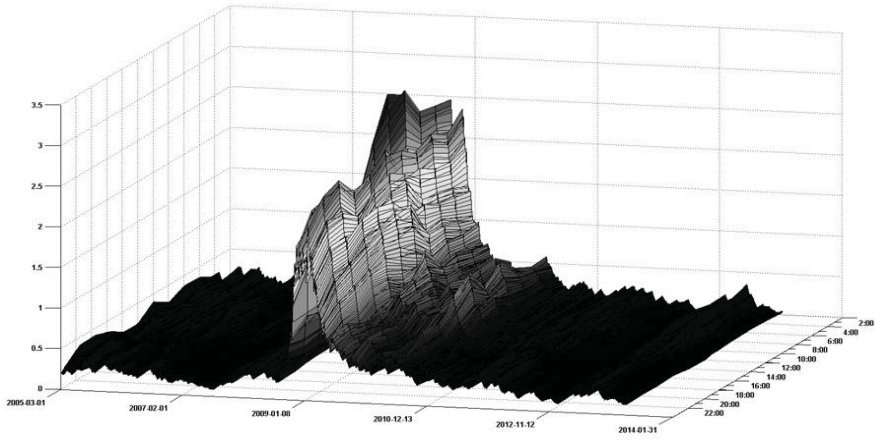

Figure 8: EUR/USD. Surface of volatilities

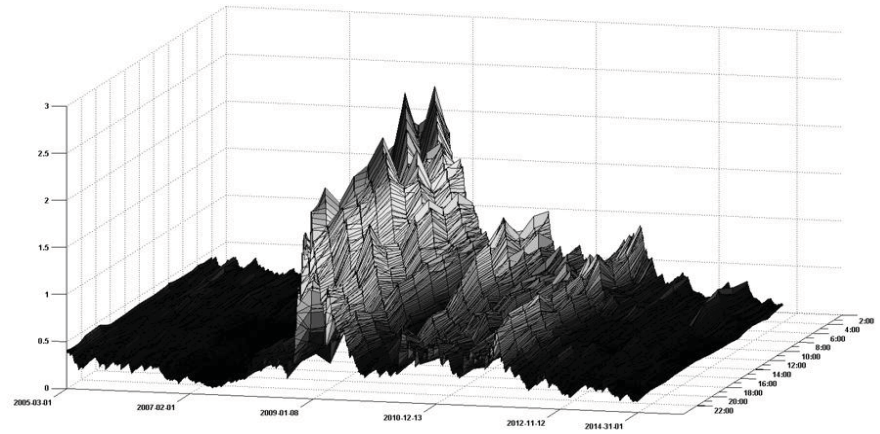

is performed for the averages of the considered exchange rate volatilities.
Tables 7-8 contain the orderings of the considered hours of a day according to the average of dynamic Spearman's rho (or the average of volatility) obtained with the MCS procedure applied sequentially. This means that after each run, the series constituting the MCS are excluded. Each block in the corresponding column (Tables 7-8) contains a model confidence set, i.e. a set of hours for which the analyzed averages are statistically indistinguishable. All the MCSs (with significance level $\alpha = 0.1$) have been estimated using the package MulCom by Hansen and Lunde (2010) written in

Table 4: Parameter estimates for MRSC models fitted to daily returns calculated for data quoted at 16:00 CET

GBP-EUR				**GBP-USD**			
GBP/USD EUR/USD	**Regime 1**	**Regime 2**	**Regime 3**	**GBP/EUR USD/EUR**	**Regime 1**	**Regime 2**	**Regime 3**
Copula	C_{ρ}^{Gauss}	C_{ρ}^{Gauss}	C^{Π}	Copula	C_{ρ}^{Gauss}	C_{ρ}^{Gauss}	$C_{\kappa,\gamma}^{Joe-Clayton}$
ρ	0.6317 (0.0242)	0.8019 (0.0098)		ρ	0.2828 (0.0270)	0.6396 (0.0211)	
κ				κ			3.5480 (0.4410)
γ				γ			2.4248 (0.6465)
Transition probabilities				**Transition probabilities**			
Regime 1	0.9925	0.0030	0.0045	**Regime 1**	0.9987	0.0013	0.0000
Regime 2	0.0030	0.9970	0.000	**Regime 2**	0.0021	0.9941	0.0038
Regime 3	0.0755	0.0000	0.9245	**Regime 3**	0.0001	0.0057	0.9422

Table 5: Parameter estimates for MRSC models fitted to daily returns calculated for data quoted at 10:00 CET

GBP-EUR			**GBP-USD**		
GBP/USD EUR/USD	**Regime 1**	**Regime 2**	**GBP/EUR USD/EUR**	**Regime 1**	**Regime 2**
Copula	C_{ρ}^{Gauss}	C_{ρ}^{Gauss}	Copula	$C_{\kappa,\gamma}^{Joe-Clayton}$	$C_{\kappa,\gamma}^{Joe-Clayton}$
ρ	0.5649 (0.0310)	0.7885 (0.0152)	ρ		
κ			κ	1.2956 (0.0392)	1.8873 (0.1025)
γ			γ	0.1302 (0.0359)	0.7871 (0.1053)
Transition probabilities			**Transition probabilities**		
Regime 1	0.9838	0.0162	**Regime 1**	0.9988	0.0012
Regime 2	0.0129	0.9871	**Regime 2**	0.0034	0.9966

Ox (Doornik 2006).

The highest level of dependence between the GBP/USD and EUR/USD is observed when the European markets are open. In the case of (GBP/EUR, USD/EUR), the strongest linkages are produced by Asian markets. For each of the considered hours the average of dynamic Spearman's rho for (GBP/USD, EUR/USD) turned out to

Table 6: Parameter estimates for MRSC models fitted to daily returns calculated for data quoted at 6.00 CET

GBP-EUR			**GBP-USD**			
GBP/USD EUR/USD	**Regime 1**	**Regime 2**	**GBP/EUR USD/EUR**	**Regime 1**	**Regime 2**	**Regime 3**
Copula	C_{ρ}^{Gauss}	C_{ρ}^{Gauss}	Copula	C_{ρ}^{Gauss}	C_{ρ}^{Gauss}	$C_{\kappa,\gamma}^{Joe-Clayton}$
ρ	0.4804 (0.0367)	0.7378 (0.0129)	ρ	0.3457 (0.0326)	0.6424 (0.0340)	
κ			κ			1.7014 (0.1259)
γ			γ			0.8926 (0.1533)
Transition probabilities			**Transition probabilities**			
Regime 1	0.9836	0.0164	**Regime 1**	0.9962	0.0038	0.0000
Regime 2	0.0086	0.9914	**Regime 2**	0.0049	0.9935	0.0016
			Regime 3	0.0037	0.0000	0.9963

be significantly higher than that for (GBP/EUR, USD/EUR). There are, however, some periods and hours when of dynamic Spearman's rho estimates show stronger dependence for the pair (GBP/EUR, USD/EUR) (Figure 14).

Figure 9: Dynamic Spearman's rhos for (GBP/USD, EUR/USD)

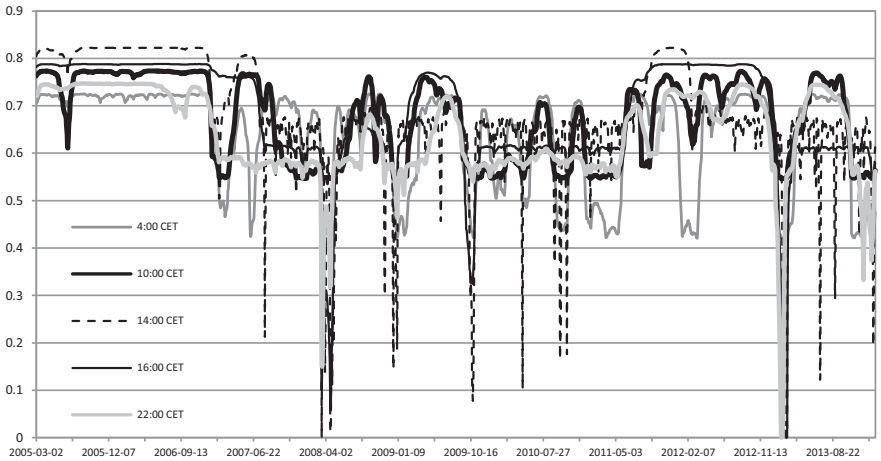

The results for volatility (Table 8) in the case of the EUR/USD and GBP/USD seem

Figure 10: Surface of dynamic Spearman's rhos for (GBP/USD, EUR/USD)

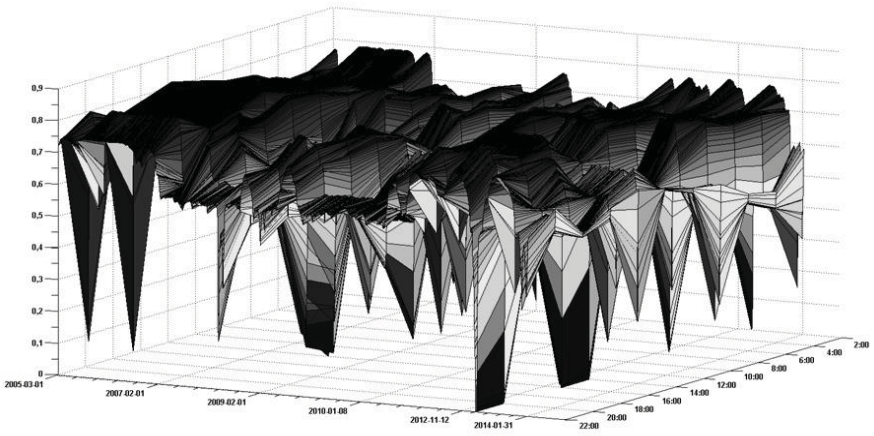

Figure 11: Dynamic Spearman's rhos for (GBP/EUR, USD/EUR)

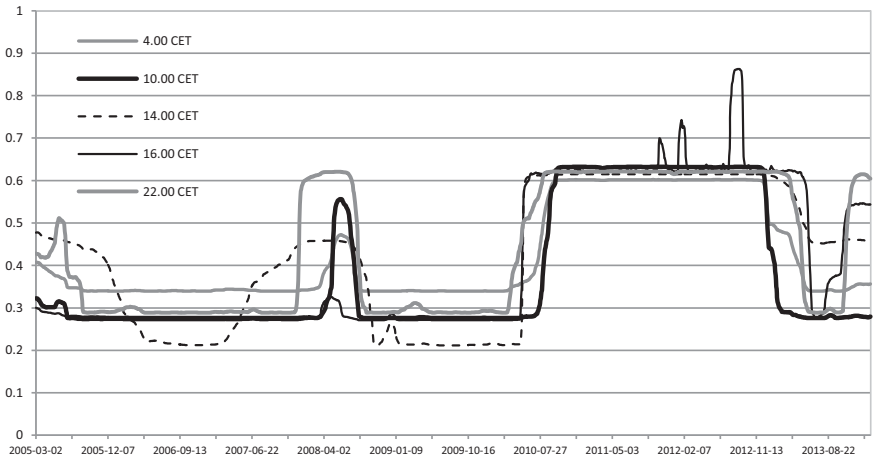

to be little surprising. The higher averages of volatility are connected with activity of Asian markets. In agreement with what we expected, the highest volatility of the GBP/EUR appears during the trade in European markets. In general, however, the results presented in Table 8 are consistent with our earlier observations. The GBP/EUR trading is mainly due to Europe. The periods of high volatility of the EUR/USD are the periods with asymmetries. The highest volatility of the GBP/USD occurs for the hours corresponding to Asian markets activity and at the beginning of trading in Europe. The lowest volatility of the EUR/USD is the one for the daily

Figure 12: Surface of dynamic Spearman's rhos for (GBP/EUR, USD/EUR)

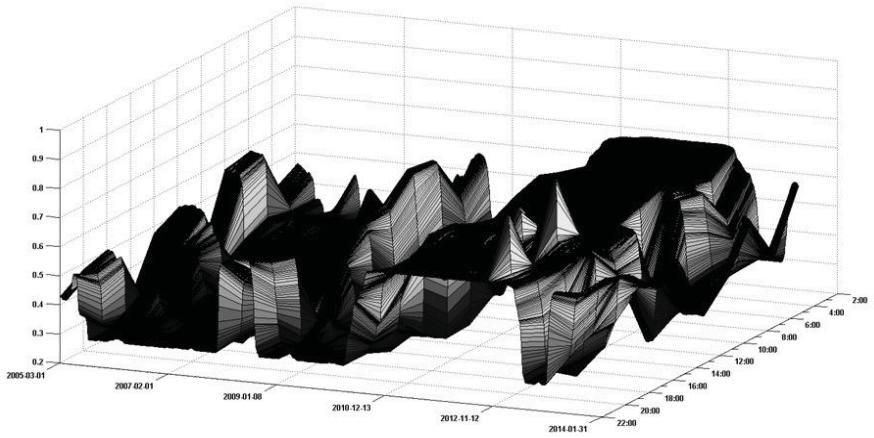

Figure 13: Dynamic coefficients of lower tail dependence for (GBP/EUR, USD/EUR)

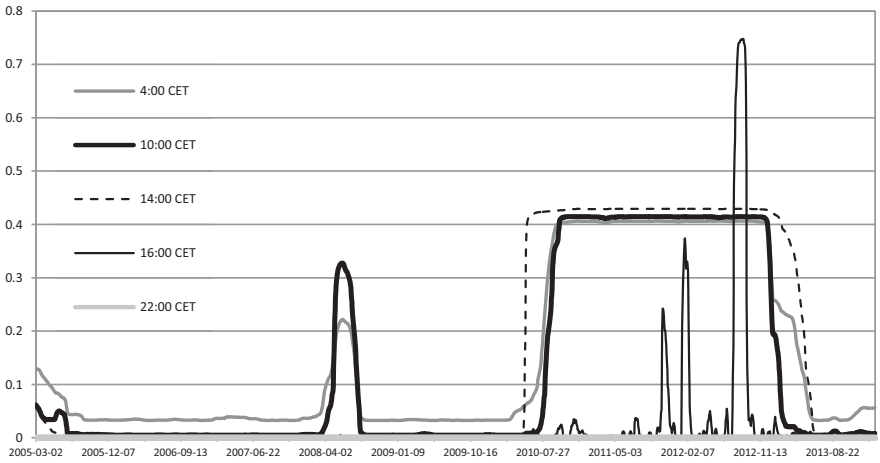

returns calculated for the data quoted at 14:00 CET and later. This might indicate that the U.S. traders are not very concerned about this exchange rate.
A comparison of the results from Tables 7 and 8 allows us to claim that the hours for which the average of strength of the dynamic linkages is maximum do not necessary agree with the hours for which the averages of the daily volatility are the highest.

Figure 14: Comparison of dynamic Spearman's rho estimates for the data quoted at 6:00 CET

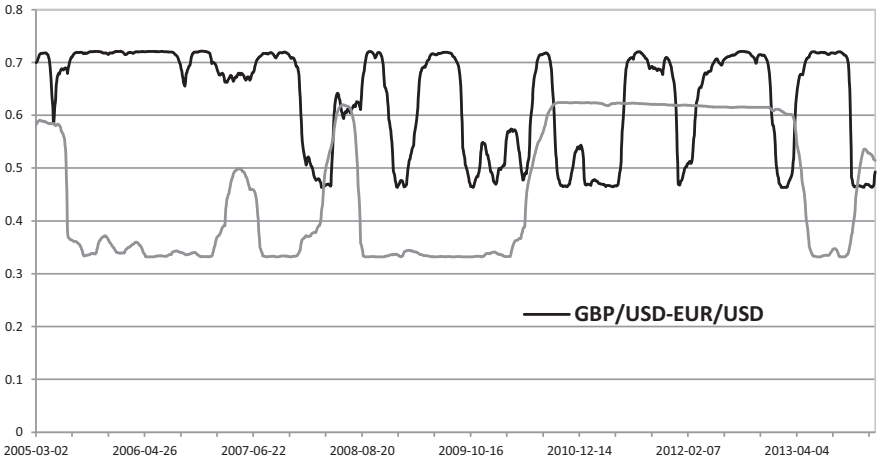

Table 7: Results of the MCS procedure applied to dynamic Spearman's rho estimates corresponding to the considered hours. Decreasing order according to the averages of strength of dependence

Average strength of linkages	GBP/USD-EUR/USD	GBP/EUR-USD/EUR
	12:00 CET 14:00 CET 16:00 CET	2:00 CET 6:00 CET
	10:00 CET	8:00 CET
↓	8:00 CET 20:00 CET	22:00 CET
	18:00 CET	4:00 CET 14:00 CET 20.00 CET
	2:00 CET	18:00 CET
	4:00 CET	12:00 CET
	22:00 CET	16:00 CET
	6:00 CET	10:00 CET

Table 8: Results of the MCS procedure applied to volatility estimates corresponding to the considered hours. Decreasing order according to the averages of volatility

Average volatility	EUR/USD	GBP/EUR	GBP/USD
↓	2:00 8:00	10:00 12:00	8:00
	4:00 12:00	6:00 8:00	2:00 6:00
	6:00 10:00	2:00 4:00 14:00 18:00	4:00 10:00
	14:00 18:00 20:00 22:00	20:00	12:00 14:00 22:00
		16:00	18:00
		22:00	20:00
			16:00

7 Conclusions

The aim of the paper was to discover the possible impact of the part of a day (and thus the activity of regional FOREX markets) on the dynamics of conditional dependencies for the pairs (GBP/EUR, USD/EUR) and (GBP/USD, EUR/USD). The analysis was based on daily returns calculated using exchange rates quoted at selected hours of a day. Volatility was estimated by means of ARMA-GARCH models. To describe changes in a pattern of linkages we applied 3-regime Markov regime switching copula models, and the strength of the dependencies was described using dynamic Spearman's rho and tail dependence coefficients.

Our findings are as follows. The dynamics of volatility estimates corresponding to different hours do not differ considerably. Nevertheless, the differences between the averages of volatility corresponding to some hours are statistically significant. The dynamics of dependencies between GBP/USD and EUR/USD shows strong sensitivity on market events. The highest level of dependence in this case is observed when European markets are open. The dynamic Spearman's rho estimates for the pair (GBP/EUR, USD/EUR) are lower than those for (GBP/USD, EUR/USD) but more stable. In the case of (GBP/EUR, USD/EUR), the strongest linkages are produced by Asian markets. For each of the considered hours we found that the average of dynamic Spearman's rho for (GBP/USD, EUR/USD) was significantly higher than

that for (GBP/EUR, USD/EUR). It also follows from our results that the hours for which the average of strength of the dynamic linkages is the highest do not necessary agree with the hours for which the averages of the daily volatility are maximum.

References

[1] Almeida C., Czado C., (2012), Efficient Bayesian Inference for Stochastic Time-Varying Copula Models, *Computational Statistics and Data Analysis* 56, 1511-1527.

[2] Doornik J.A., (2006), *An Object-oriented Matrix Programming Language* – Ox^{TM}, Timberlake Consultants Ltd, London.

[3] Eun C.S., Lai S.S., (2004), *The Currency Co-movement*, Georgia Institute of Technology Working Paper 21.

[4] Eun C., Lai S., Lee K., (2013), *Exchange Rates Comovement*, KAIST Business School Working Paper Series, KCB-WP-2013-020.

[5] Garcia R., Tsafack G., (2011), Dependence Structure and Extreme Comovements in International Equity and Bond Markets, *Journal of Banking & Finance* 35 (8), 1954-1970.

[6] Hamilton J.D., (1994), *Time Series Analysis*, Princeton University Press, Princeton.

[7] Hansen P.R., Lunde A., Nason J.M., (2003), Choosing the Best Volatility Models: The Model Confidence Set Approach, *Oxford Bulletin of Economics and Statistics* 65, 839–861.

[8] Hansen P.R., Lunde A., (2010), MulCom 2.00, an Ox^{TM} Software Package for Multiple Comparisons, `http://mit.econ.au.dk/vip_htm/alunde/mulcom/mulcom.htm`

[9] Hansen P.R., Lunde A., Nason J.M., (2011), The Model Confidence Set, *Econometrica* 79 453–497.

[10] Joe H., (1997), *Multivariate Models and Dependence Concepts*, Chapman and Hall, London.

[11] Laurent S., (2009), *Estimating and Forecasting ARCH Models Using* G@RCH 6, Timberlake Consultants, London.

[12] McNeil A.J., Frey A., Embrechts P., (2005), *Quantitative Risk Management*, Princeton University Press, Princeton.

[13] Min A., Czado C., (2010), Bayesian Inference for Multivariate Copulas Using Pair-Copula, Constructions, *Journal of Financial Econometrics* 8, 511-546.

[14] Nelsen R.B., (2006), *An Introduction to Copulas*, Springer, New York.

[15] Patton A.J., (2004), On the Out-of-Sample Importance of Skewness and Asymmetric Dependence for Asset Allocation, *Journal of Financial Econometrics* 2, 130-168

[16] Patton A.J., (2006), Modelling Asymmetric Exchange Rate Dependence, *International Economic Review* 47 (2), 527-556.

[17] Patton A.J., (2012), A Review of Copula Models for Economic Time Series, *Journal of Multivariate Analysis* 110, 4-18.

[18] Patton A.J., (2013), Copula Methods for Forecasting Multivariate Time Series, Chapter 17, [in:] *Handbook of Economic Forecasting*, Vol. 2B [ed.:] G. Elliott, A. Timmermann, North-Holland, 899-960.

[19] Sklar A., (1959), Fonctions de répartition à n dimensions et leurs marges, *Publications de l'Institut Statistique de l'Université de Paris* 8, 229-231.

[20] Triennial Central Bank Survey, (2013), Foreign exchange turnover in April 2013: preliminary global results, Monetary and Economic Department, Bank for International Settlements, (available at `http://www.bis.org/publ/rpfx13fx.pdf`).

[21] Tsay R.S., (2010), *Analysis of Financial Time Series*, Wiley, Hoboken.